Available online at www.sciencedirect.com
SCIENCE DIRECT
polymer
Polymer 47 (2006) 23–26
www.elsevier.com/locate/polymer

Polymer Communication

# Facile synthesis of metal nanoparticles using conducting polymer colloids

Wenguang Li [a], Q.X. Jia [b], Hsing-Lin Wang [a,*]

[a] *MSJ-586, Physical Chemistry and Spectroscopy group, Chemistry Division, Los Alamos National Laboratory, Los Alamos, NM 87545, USA*
[b] *MSK763, Materials Science and Technology Division, Los Alamos National Laboratory, Los Alamos, NM 87545, USA*

Received 5 August 2005; received in revised form 10 November 2005; accepted 11 November 2005
Available online 28 November 2005

**Abstract**

We report a simple method to synthesize Ag, Au, and Pt nanoparticles with a reasonable size dispersity using water-dispersible conducting polymer colloids composed of polyaniline (PANI) and conventional polyelectrolyte. This facile synthesis results in single crystalline metal nanoparticles that are stable in an aqueous solution for at least several weeks. The process involves incrementally adding a metal ion solution to aqueous conducting polymer colloids and does not require reducing agents such as $NaBH_4$. In addition, the complete synthetic and purification procedure is carried out in an aqueous solution; therefore, it is environmentally benign and potentially suitable for large-scale production. We have also demonstrated synthesis of larger nanoparticles and nanosheets by varying the experimental parameters. With the tunable oxidation states of conducting polymers, we expect this synthetic platform can synthesize a wide range of nanostructured metals with specific size, shape and properties. Finally, the nanoparticles embedded in the conducting polymer matrix, the metal–polyaniline nanocomposite itself may be interesting since it represents a type of materials where metallic nanoislands are embedded in a semiconducting matrix.


*Keywords:* Conducting polymer; Metal nanoparticles; Synthesis

The synthesis of metal nanoparticles has sparked intense interest because of their potential use as catalysts [1,2], absorbents [3], chemical [4], and biological [5] sensors, as well as photonic [6,7] and electronic [8] devices. Traditionally, such a synthesis is carried out chemically with a reducing agent such as $NABH_4$ or with irradiation used to convert groups of metal ions into nanoparticles. In essence, metal ions are reduced in the presence of a template and/or stabilizer, which draws nearby metal ions together, thereby, forming nanoparticles [9–12]. To grow nanoparticles, inverse micelles were used, but this process suffers from low yield and low stability in the air–oxygen environment [13]. Known for their ability to reduce metal ions, conducting polymers have demonstrated the potential for the metallization of printed circuit boards [14] and the recovery of Au by electrodeless precipitation [15]. More recently, Au nanoparticles as small as 20 nm were prepared by adding $AuCl_3$ to a polyaniline (PANI) solution [16]. However, using conducting polymers to reduce metal ions to form metal nanoparticles results in nanoparticles with a relatively large particle size and poor size distribution. In addition, these as prepared nanoparticles are not dispersible in most common solvents. To mitigate this problem, Zhou et al. reduced metals ions by using polydithiafulvene (PDF), a process that results in stable metal nanoparticles coated with oxidized PDF [17]. Despite all the above efforts, there has been limited success in preparing some of the metal nanoparticles, and most procedures often require size-selective precipitation to obtain high quality metal nanoparticles. For this reason, it is also very costly to purchase the commercially available polycrystalline Au nanoparticle with only a reasonable particle size distribution. It is obvious that for scientific and commercial reasons, a need remains for a facile, large-scale, environmentally friendly process that synthesizes metal nanoparticles.

In this communication, we report a simple method to synthesize single crystalline Ag, Au, and Pt nanoparticles with a good size dispersity by using water-dispersible colloids composed of PANI and conventional polyelectrolytes such as polyacrylic acid (PAA). This PANI colloid consists of a spherical outer layer that is PAA rich and an inner core that is a homogeneous mixture of PANI and PAA [18]. The colloidal particles of PAA–PANI range in size between 100 and 150 nm (Fig. 1(A)). In the synthesis of metal nanoparticles, PANI is the reducing agent. PAA not only makes the colloidal particles

* Corresponding author.
*E-mail address:* hwang@lanl.gov (H.-L. Wang).

0032-3861/$ - see front matter © 2005 Elsevier Ltd. All rights reserved.
doi:10.1016/j.polymer.2005.11.032

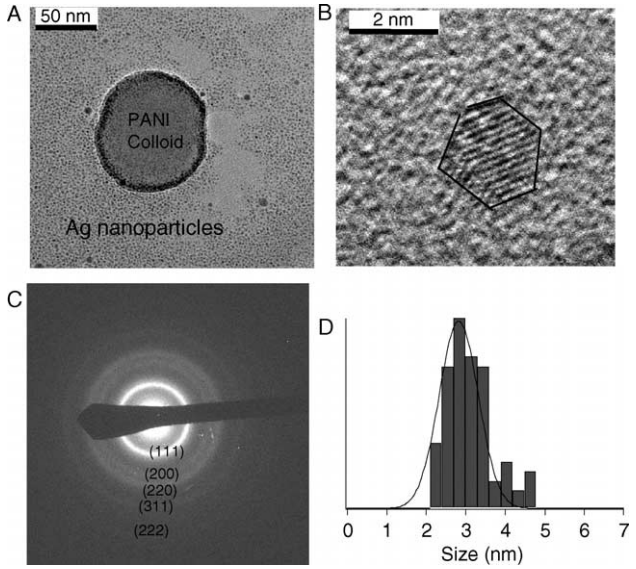


Fig. 1. (A) A TEM micrograph showing an undoped PANI colloid and homogeneously dispersed Ag nanoparticles. (B) Magnification of the Ag nanoparticles. (C) Graph showing the electron diffraction of an ensemble of Ag nanoparticles. (D) Size distribution histogram of the Ag nanoparticles.

hydrophilic, but it also binds and pulls metal ions to the PANI colloids. The reduction of metal ions takes place either within the colloidal particles or on the surface of the nanoparticles. The PANI colloidals actually act as tiny reactors. Synthesizing Ag nanoparticles was achieved by adding a metal ion aqueous solution to a PANI colloid solution. The synthetic procedure of preparing Ag nanoparticles by using undoped PANI colloids is as follows. Every 2 h, 0.05 ml of 30 mM $AgNO_3$ is added to 1.0 ml of 1.8 wt% PAA–PANI colloidal dispersion, which is equivalent to 20 mM PANI, until 1.4 ml of $AgNO_3$ is added. The solution is stirred overnight to ensure the complete reduction of $Ag^+$. The final step involves dialyzing the Ag nanoparticles and PANI colloid solution against DI water by using a tubular membrane with a molecular weight cut off (MWCO) at 3500 Da to remove the excess ionic residue.

The TEM micrograph of the as-synthesized Ag nanoparticles shows that most nanoparticles are dispersed homogeneously in the solution with some nanoparticles residing at the periphery of the PANI colloid. The Ag nanoparticles appear to form a shell about 10 nm thick around the surface of the PANI colloidal particles (Fig. 1(A)). The core structure of the PANI colloid is free from Ag nanoparticles. This result suggests that the reduction of silver ions takes place exclusively on the periphery of the PANI colloidal particles. The high-resolution TEM micrograph also shows that most of the nanoparticles have clear crystalline planes aligned along a specific direction. An example of a 2 nm Ag single crystalline nanoparticle is shown in Fig. 1(B). Fig. 1(C) shows the electron diffraction of an ensemble of the as-synthesized Ag nanoparticles. The diffraction spots of Ag nanoparticles with a random crystalline orientation result in the formation of ring patterns. The ring patterns are identified to be (111), (200), (220), (311), and (222). The broadening of the ring patterns, typically observed in extremely small particles, is consistent with the electron

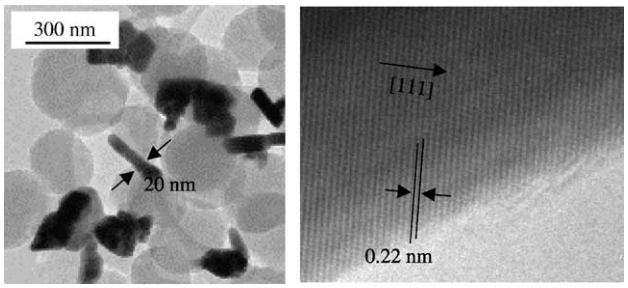


Fig. 2. TEM micrograph of undoped PANI colloids and Ag nanosheet (left) and high resolution TEM on the edge of a silver nanosheet (right).

diffraction pattern observed in our Ag nanoparticles. We can therefore, conclude from the TEM micrographs and electron diffraction that the final products are indeed Ag nanoparticles. These Ag nanoparticles also exhibit good stability. For example, they remain dispersed in an aqueous solution for several weeks before they start to settle at the bottom of the container. However, we can easily redisperse these nanoparticles by simply shaking the container. The size dispersity is determined by analyzing the particle-size distribution directly from the TEM image. The histogram of ~200 Ag nanoparticles is shown in Fig. 1(D). The high resolution TEM of Ag nanoparticle shows that 75% of these as-synthesized Ag nanoparticles have a size distribution that ranges from 2.5 to 3.5 nm.

Synthesizing Ag nanoparticles requires careful control of the reaction parameters such as the relative concentration between PANI colloids and $AgNO_3$ and the rate of mixing. Increasing the concentration of $AgNO_3$ leads to the formation of larger nanostructured Ag. Adding all of the $AgNO_3$ solution to the PANI dispersion at one time also results in the formation of larger silver nanosheets up to 250 nm (Fig. 2(A)). These nanosheets have a thickness of ~20 nm. The high-resolution TEM shows that these nanosheets are also single crystalline. Only through the incremental addition of 0.05 ml of 30 mM $AgNO_3$ every 2 h with constant stirring, can we generate Ag nanoparticles with a good size distribution (2–4.5 nm). Although our preliminary study shows that some large metal structures exist in the solution, the as-synthesized Ag nanoparticles are largely single crystalline and have a good size dispersity. Separation and purification of these nanoparticles by centrifugation can remove the larger unwanted structures to improve the size dispersity.

In another experiment, we use nitric acid doped PANI colloids instead of undoped PANI colloids to synthesize Ag nanoparticles by following the same procedure. Rather than dispersing throughout the solution, all of the as-synthesized Ag nanoparticles reside strictly within the core of the PANI (Fig. 3(A)). Obtaining an electron diffraction of Ag nanoparticles in this instance proved difficult because all of the Ag nanoparticles were buried within the inner portion of the PANI colloids. Therefore, we measured the X-ray diffraction of the as-cast thin film from the Ag–PANI colloid solution and confirmed the existence of the Ag nanoparticles (Fig. 3(B)). The broadening of the X-ray diffraction peaks caused by the

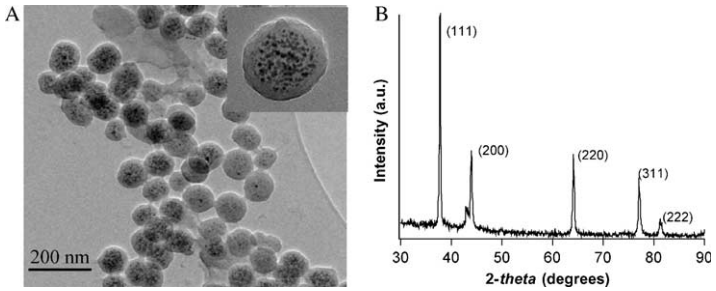


Fig. 3. TEM micrograph shows Ag nanoparticles homogeneously dispersed within doped PANI colloids (A), and (B) X-ray diffraction of a thin film cast from a solution that consists of PANI colloids and Ag nanoparticles.

size of the Ag nanoparticle is consistent with the results reported for the nanocrystalline materials [19]. The average size of these nanoparticles, calculated from the diffraction line breadths due to the particle size effect, is about 17 nm. This value is much larger than what we see from TEM analysis (Figs. 1(B) and 3(A)). We believe that the large particles (Fig. 1 (A)), though they are sparsely distributed along with much smaller nanoparticles, dominate mostly the X-ray diffraction patterns. This striking difference between the as-synthesized Ag nanoparticles using doped and undoped PANI colloids is of great interest. The as-synthesized Ag nanoparticles using undoped PANI colloids appear to disperse homogeneously throughout the aqueous solution with some nanoparticles reside at the periphery of the PANI colloid, whereas the Ag nanoparticles prepared using doped PANI colloids are formed within the PANI colloids results in a hybrid metal–polymer composite. Such difference can be explained by the charges on the polymer chains and the counter ions (dopants) that open the pores in the doped PANI colloids. As the pores open, metal ions diffuse into the core of the PANI colloids and get reduced to form nanoparticles. As for the undoped PANI colloids, most metal ions are reduced on the surface of the PANI colloids, which then disperse throughout the solution. This result is consistent with previous studies, which show that the incorporation of dopants increases the membrane pore size, thus allowing the facile diffusion of larger molecules [20,21]. Another possible explanation is that such a difference is caused by PAA, which is in the form of COO– in undoped PANI colloids, and in the form of COOH in doped PANI colloids. Because $COO^-$ can bind silver ions more tightly than COOH can, Ag ions do not diffuse through the PAA rich layer to reach the core of the PANI colloid.

Reducing the metal ions to form metal nanoparticles by using undoped PANI colloids is further confirmed by monitoring the PANI's oxidation states during the synthesis by using UV–vis spectroscopy. As the metal ions are reduced, we observe the formation of a new peak at ~300 nm and a blue shift (from 630 to 570 nm) of the exciton peak in the PANI's UV–vis spectrum. The changes in the UV–vis spectra of PANI colloids directly reflect changes in the PANI component because PAA does not have absorption at this region (250–800 nm). This result suggests that PANI's oxidation state changes from the emeraldine base to the fully oxidized pernigraniline base [22]. These changes are depicted in Scheme 1. Each PANI repeating unit can convert two single-charged metal ions into two metal atoms. We speculate that the formation mechanisms of Ag nanoparticles, which are similar to those proposed by Finke et al. [23] suggesting that the ratio of rate of growth to nucleation, $R(=K2[\text{nanocluster active sites}]/K1[\text{nucleation}])$, should correlate with and therefore, be a useful parameter to predict the size of the nanoparticles. The incremental addition of the metal ion solution to the PANI solution allows the formation of a relatively larger number of nuclei and also fort the quenching of the surface growth at the early stage of the nanoparticle formation. This hypothesis appears to be consistent with our experimental results. Further kinetic study will be carried out to validate this hypothesis.

Consequently, we use a similar procedure to synthesize Au nanoparticles by using undoped and doped PANI colloids. In this experiment, the as-synthesized Au nanoparticles either aggregated at the outer surface of the undoped PANI colloids or were trapped within the doped PANI colloids (Fig. 4(A) and (B)). The average size of the Au nanoparticles is estimated to be ~7–12 nm. It is difficult to estimate the size dispersity of these Au nanoparticles because they tend to form aggregates. The presence of Au nanoparticles is confirmed by XRD, in which (111), (200), (220), (311), and (222) peaks have been identified (Fig. 4(C) and (D)). We also observed a broadening

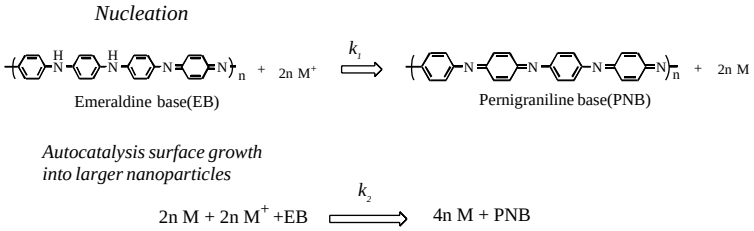


Scheme 1. Minimum mechanism for the formation of metal nanoparticles consisting of nucleation step (rate constant $K1$) followed by fast autocatalytic surface growth (rate constant $K2$).

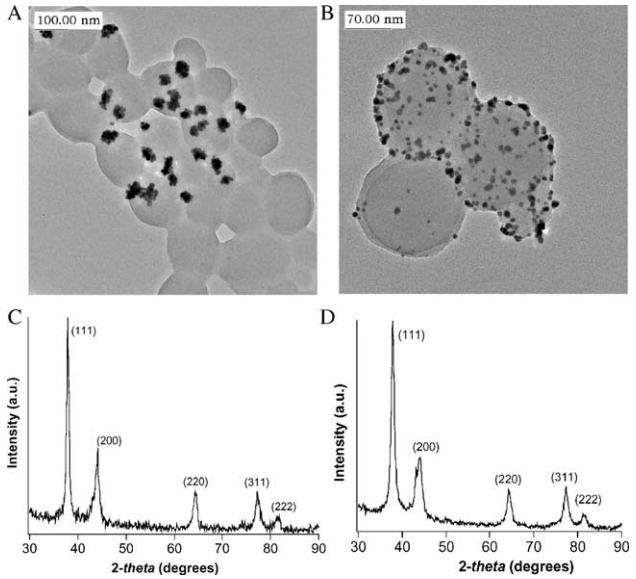


Fig. 4. The top two micrographs show Au nanoparticles synthesized using (A) undoped PANI colloids and (B) doped PANI colloids. The bottom two graphs (C) and (D) show X-ray diffraction spectra of thin films cast from solution (A) and (B), respectively.

of the XRD peaks caused by the size of the Au nanoparticles. The TEM micrograph of an 11 nm single crystalline Au nanoparticle, half buried in a PANI colloidal, is shown in Fig. 5. It should be noted that the particle size calculated based on the extra breadth or broadening due to the particle-size effect alone from X-ray diffraction lines is about 12 nm, which agrees extremely well with the TEM results. This is expected considering much uniformly distributed Au nanoparticles. The crystalline plane at the [111] direction is clearly observed and the distance between the crystalline planes is calculated from the fast Fourier transforms (FFT) of this Au nanoparticle and is determined to be 2.3 Å, a distance consistent with the lattice parameters of the Au metal.

Furthermore, we have demonstrated the synthesis of Pt nanoparticles. The TEM micrograph of a single crystalline 2 nm-Pt nanoparticle shows crystalline planes of (200), (111), and (11$\bar{1}$) (Fig. 5). The distances between the crystalline planes determined by FFT are 1.98, 2.29 and 2.29 Å, respectively. This result is consistent with the lattice parameters of a Pt metal. In addition, the angles between the crystalline facets are determined to be 54.5° between (200) and (111), and 70.3° between (111) and (11$\bar{1}$). These two angles match well with the hexagonal crystalline facets usually occurring at low-index (low-energy) surfaces.

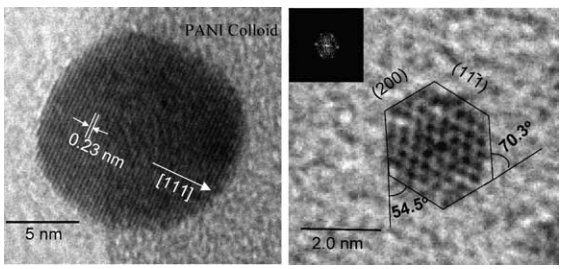


Fig. 5. HRTEM of a single crystalline Au nanoparticle (left) and Pt nanoparticle (right), inset shows the FFT of Pt nanoparticle.

It should also be noted that the polypyrrole colloids and polythiophene dispersion- (trade name: Baytron P, Bayer Co.) are also being used to synthesize Ag and Au nanoparticles by following the same procedure described previously. Preliminary results show that the as-synthesized Ag and Au nanoparticles are not single crystalline and have larger nanoparticle sizes, ranging from 5 to 40 nm. Although the detailed kinetics of forming metal nanoparticles by using conducting polymer colloids remained unclear, the PANI-based synthesis of narrowly dispersed, single crystalline metal nanoparticles provides a novel synthetic platform that is versatile, environmentally benign and suitable for large-scale production. The tunable redox states of PANI are also expected to provide another level of control to synthesize a wide range of nanostructure metals with specific size, shapes, and properties.

## Acknowledgements

The authors would like to thank Dr Huifang Xu and Mr Ying-Bing Jiang at the University of New Mexico for the assistance in TEM. The work is supported by the LDRD program of Los Alamos National Laboratory, and the office of Basic Energy Science (DOE).

## References

[1] Lewis LN. Chem Rev 1993;93:2693–730.
[2] Ahmadi TS, Wang ZL, Green TC, Henglein A, ElSayed MA. Science 1996;28:1924–6.
[3] Thomas JM. Pure Appl Chem 1988;60:1517–28.
[4] Emory SR, Nie S. J Phys Chem B 1998;15:493–7.
[5] Templeton AC, Cliffel DE, Murray RW. J Am Chem Soc 1999;4:7081–9.
[6] Zhong ZY, Gates B, Xia YN, Qin D. Langmuir 2000;16:10369–75.
[7] Maier SA, Brongersma ML, Kik PG, Meltzer S, Requicha AAG, Atwater HA. Adv Mater 2001;2:1501.
[8] Feldheim DL, Keating CD. Chem Soc Rev 1998;27:1–12.
[9] Zheng J, Dickson RM. J Am Chem Soc 2002;27:13982–3.
[10] Crooks RM, Zhao MQ, Sun L, Chechik V, Yeung LK. Acc Chem Res 2001;34:181–90.
[11] Sidorov SN, Bronstein LM, Valetsky PM, Hartmann J, Colfen H, Schnablegger H, et al. J Colloid Interface Sci 1999;212:197–211.
[12] Mayer ABR, Mark JE. Polymer 2000;41:1627–31.
[13] Petit C, Lixon P, Pileni MP. J Phys Chem 1993;9:12974–83.
[14] Huang WS, Angelopoulos M, White JR, Park JM. Mol Cryst Liq Cryst 1990;189:227–35.
[15] Ting YP, Neoh KG, Kang ET, Tan KL. J Chem Technol Biotechnol 1994; 59:31–6.
[16] Wang JG, Neoh KG, Kang ET. J Colloid Interface Sci 2001;1:78–86.
[17] Zhou Y, Itoh H, Uemura T, Naka K, Chujo Y. Langmuir 2002;8:277–83.
[18] Li W, Hooks DE, Chiarelli PA, Jiang Y, Xu H, Wang HL. Langmuir 2003; 19:4639.
[19] Indris S, Heitjans P, Roman HE, Bunde A. Phys Rev Lett 2000;27: 2889–92.
[20] Anderson MR, Mattes BR, Reiss H, Kaner RB. Science 1991;252:1412–5.
[21] Anderson MR, Mattes BR, Reiss H, Kaner RB. Synth Met 1991;41: 1151–4.
[22] Wei Y, Focke WW, Wnek GE, Ray A, Macdiarmid AG. J Phys Chem 1989;93:495–9.
[23] Watzky M, Finke R. Chem Mater 1997;9:3083–95.